

18 CM OH-LINE RADIATION FROM NGC 6334

By F. F. GARDNER,* R. X. MCGEE,* and B. J. ROBINSON*

[Manuscript received December 20, 1966]

Summary

A survey of the OH-line radiation from the region of NGC 6334 has been made with the Parkes 210 ft telescope (beamwidth $12' \cdot 2$ arc, bandwidth 10 kHz). Observations of both circular and linear polarization were made at 1665 MHz, and less completely at 1667 MHz.

Two centres of OH-line emission, A and B, are clearly distinguished, one on either side of the nebulosity. Each centre may consist of three or more neighbouring regions with radial velocities in the range -6 to $-12 \cdot 5$ km/sec. OH-line absorption observed at radial velocities of $-4 \cdot 5$ and $+5 \cdot 5$ km/sec probably takes place in gas complexes between the nebula and the Sun.

Strong circular polarization is present, especially in A, the more northern source, but the polarization characteristics of the two main centres are markedly different. Linear polarization is less than 10% for A. There is no clear evidence for secular variation of the line intensities.

I. INTRODUCTION

Initial studies have revealed anomalies in the observed intensity ratios for the four interstellar microwave lines of the hydroxyl molecule. Highly polarized, narrow band emission, particularly at 1665 MHz, has been found to originate from small areas within certain HII regions.

This paper is concerned with a study of the emission from a group of nebulae, some 40 min of arc in diameter, known as NGC 6334. Weaver *et al.* (1965) discovered both emission and absorption in the direction of NGC 6334 at 1665 and 1667 MHz. McGee *et al.* (1965) observed emission also at 1720 MHz and absorption at all four frequencies; they found that the main source of emission at 1665 MHz was of small angular extent and located towards the edge of the group of nebulae.

Further results were reported by Dieter, Weaver, and Williams (1966), Weaver, Williams, and Dieter (1966), and Williams, Dieter, and Weaver (1966). Six centres of emission were located; the lines at 1665 and 1667 MHz were observed to vary in intensity over periods of weeks; strong linear polarization approaching 100% was reported, and this polarization itself was reported to vary in intensity and position angle during the period of their observations. In contrast, Barrett and Rogers (1966) stated briefly that the OH-emission was strongly circularly polarized.

In the present investigation the whole area near NGC 6334 has been surveyed with the Parkes radio telescope. Subsequent to this mapping, measurements of linear and circular polarization were made at certain points in the nebula. The observations were made with a bandwidth of 10 kHz, which is considerably wider than the 2 kHz of Weaver *et al.* (1965) and Weaver, Williams, and Dieter (1966).

* Division of Radiophysics, CSIRO, University Grounds, Chippendale, N.S.W.

However, the angular resolution of the present observations is higher, with a beamwidth of $12' \cdot 5$ arc as against $30'$ arc. For this reason, our main concern has been a detailed study of the angular distribution of the emission across the nebula.

II. EQUIPMENT

(a) Feeds for the 210 ft Telescope

The observations were made with the 210 ft radio telescope of the Australian National Radio Astronomy Observatory, using two different feed arrangements: feed 1, which accepted one plane of polarization, and feed 2, with provision for accepting both planes of polarization. The 2 m diameter focal plate supporting the feed system can be rotated, but all observations with feed 1 were made for fixed polarization with the electrical field vertical. Because the parallactic angle changes slowly with an altitude–azimuth drive (see Gardner and Davies 1966, Fig. 2), the position angle of polarization varied slowly during a set of observations. With feed 2 the position angle of polarization was kept constant to an accuracy of about one degree by a servo system driven from the telescope's analogue controller, "the master equatorial".

(i) Feed 1; Rectangular Horn

The earlier OH-line observations were all made with this feed, which produces an approximately circular beam with a half-intensity width of $12' \cdot 2$ arc.

(ii) Feed 2; Circular Horn

This was a dual-mode feed system in which TE_{11} and TM_{11} modes were combined with the correct phase and amplitude at the radiating aperture to produce equal E and H plane feed patterns with low spillover. Two orthogonal waveguide-to-coaxial transducers were placed in the narrower section of the circular guide (where only the TE_{11} mode can propagate). A beamwidth of $12' \cdot 5$ and slightly lower aerial efficiency resulted from the increased illumination taper.

Determinations of linear polarization were carried out by switching between orthogonal polarizations with a diode switch. Relevant parameters were:

Isolation between orthogonal outputs	> 40 dB
Diode switch, forward attenuation	0.2 dB
reverse isolation	40 dB
standing wave ratio	< 1.3 dB

In measurements of circular polarization the orthogonal polarizations were combined with an adjustable phase difference in a hybrid junction. Right-handed and left-handed circular polarizations (RHC and LHC respectively) appear at the two output ports of the hybrid; the required port was connected to the receiver and the other was resistively terminated. The system was checked by radiating a linearly polarized signal from the centre of the paraboloid and rotating the feed platform. The rejection of the unwanted sense of circular polarization was greater than 26 dB in each case.

(b) Front Ends

Double sideband crystal-mixer receivers were used throughout. The unit incorporated with feed 1 had an overall noise temperature of $\sim 350^\circ\text{K}$ (d.s.b.); for the feed 2 combination the noise temperature was $\sim 400^\circ\text{K}$.

The local oscillator frequency was switched between a value appropriate to the OH-line frequency and a reference frequency 2.16 MHz away for all types of measurements except those of linear polarization mentioned in Section II(a)(ii). The final units in the front-end packages were 29 MHz i.f. preamplifiers of approximately 7.5 MHz bandwidth.

(c) Local Oscillators

Two frequency conversions — to 29 and to 6.7 MHz — were used before detection. The first local oscillator frequencies were derived from two tunable Clapp oscillators operating near 7 MHz. A change in Clapp frequency of 10 Hz changed the local oscillator frequency by 2.16 kHz.

The second local oscillator was a separate crystal-controlled transistor oscillator at 36.376 MHz.

(d) The Back End

Details of this part of the receiver have been given by McGee and Murray (1963). The output of the 6.7 MHz i.f. amplifier is divided into 48 channels, each of which incorporates a filter, a second detector, and a synchronous detector. The outputs are sampled and recorded in analogue and digital form. In the present experiment 32 medium band channels of double-tuned LC circuits (bandwidth 37 kHz, separation 33.2 kHz) were combined with 15 channels of 10 kHz bandwidth containing crystal filters. The medium band channels were useful in search observations and in indicating zero levels outside the line radiation. The 10 kHz channels supplied the OH-line information used in this paper.

*(e) Calibration**(i) Frequency Calibration*

Frequency monitoring of the local oscillators was carried out sufficiently often for frequency errors to be equivalent to less than ± 0.5 km/sec (1 km/sec = 5.55 kHz at 1665 MHz) in radial velocity. The monitored frequencies, together with the telescope positional information, enabled the observed radial velocities to be converted to values referred to the local standard of rest. The rest frequencies of the two main OH-lines were taken as 1665.401 and 1667.357 MHz.

(ii) Intensity Calibration

The observational records were calibrated with noise lamp signals fed through a directional coupler at the receiver input. These were related back to a fundamental calibration derived from the measured aerial beam patterns and the continuum radiation of the unpolarized radio source, Hydra A. At 1666 MHz the antenna temperature for Hydra A was taken as 24.5°K with feed 1, corresponding to an equivalent point source flux of $36 \times 10^{-26} \text{ W m}^{-2} (\text{c/s})^{-1}$ and a flux/temperature ratio

of 1.47 (see Bolton, Gardner, and Mackey 1964). The signal and image ratios were accurately determined, and it is sufficient for the purposes of this paper to regard them as equal. The noise lamp deflection was equivalent to 34°K of aerial temperature for OH-line radiation.

The noise lamp was modulated by the 385 Hz square wave for the calibration signal for frequency-switched observations with linear or circular polarization. In linear polarization switching, a directional coupler was inserted between one polarized input and the diode switch.

(iii) *Noise Fluctuations*

Several measurements were made of the r.m.s. fluctuation level for each channel. Some 20 to 70 profiles were recorded in each set with the telescope pointing to a region of apparent zero line intensity. The "average" r.m.s. noise level in a single profile computed for each channel was ± 0.7 degK for the 37 kHz bandwidth and ± 2.0 degK for the 10 kHz bandwidth. Each observation on NGC 6334 consisted of four data and four reference region profiles (one profile required 2 min to record) to give an r.m.s. noise fluctuation value of ± 1.4 degK for the 10 kHz channels. If the bandwidth of the line signal is less than 10 kHz, this value will, of course, increase.

III. METHODS OF OBSERVATION

A general mapping of the 1665 MHz line emission, with a grid of points at intervals of 5 min of arc in declination and 30 sec in right ascension, was made with the feed 1 system. Some intermediate points were added where the intensities were high.

The 1667 MHz line emission was similarly mapped, but in view of the knowledge gained from the first set only half the number of points were included.

Measurements of circular and linear polarization were made over a restricted series of points mainly at the frequency of the 1665 MHz line.

(a) *Polarization Determination*

The alternative specifications of the polarization of noncoherent radiation with the definition of the Stokes parameters I , Q , U , and V have been discussed by Gardner and Whiteoak (1966). Our basic observations are of the circularly polarized intensities I_{RHC} and I_{LHC} and of the difference between orthogonal linearly polarized intensities. Right-handed circular polarization corresponds to clockwise rotation looking along the direction of travel.

The degree of circular polarization r is given by

$$r = (I_{\text{RHC}} - I_{\text{LHC}}) / (I_{\text{RHC}} + I_{\text{LHC}}) = V/I. \quad (1)$$

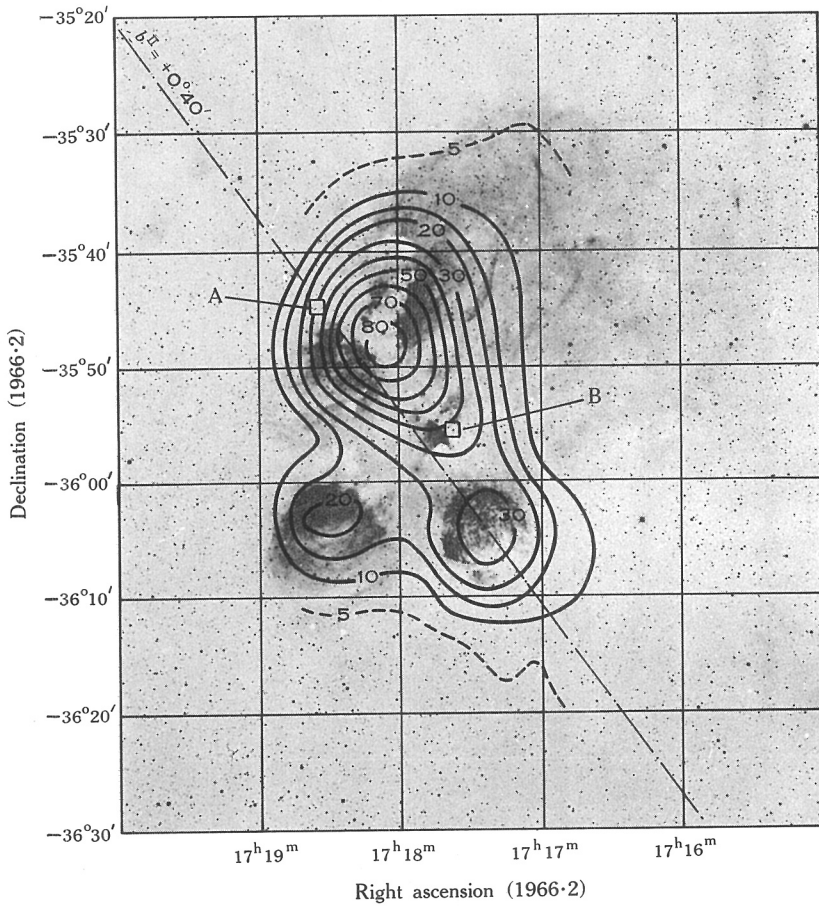
Errors from the finite rejection of the unwanted circular polarization (> 26 dB) are negligible, except when the degree of linear polarization of the incoming radiation is very high. To allow for this possibility, the circularly polarized observations were all made at a fixed position angle of the feed so that any contribution from linear

18 CM OH-RADIATION FROM NGC 6334



Photograph of NGC 6334 reproduced from a 60 min exposure in $H\alpha$ light by Dr. C. Roslund with the 20/26 in. Schmidt telescope of the Uppsala Southern Station.

18 CM OH-RADIATION FROM NGC 6334



Continuum contours at wavelength 11.3 cm are superimposed on the photograph of the nebula NGC 6334. The half-intensity beamwidth of the aerial was $7'.5$ arc. Units of intensity are relative only. The positions of OH-line emission sources A and B are indicated.

polarization would be constant. As the axial ratios and orientation of the elliptical antenna patterns had been measured in the calibration procedure, a correction could have been applied, if necessary, after the linear polarization had been subsequently determined.

For the determination of linear polarization, feed 2, the dual-polarization feed, was set at position angles 0° , 90° , 45° , and 135° , where it measured in turn

$$\left. \begin{aligned} I_0 - I_{90} &= Q, & I_{90} - I_{180} &= -Q, \\ I_{45} - I_{135} &= U, & I_{135} - I_{225} &= -U. \end{aligned} \right\} \quad (2)$$

The differences of the pairs 0° , 90° and 45° , 135° then give $2Q$ and $2U$ respectively. Combining in pairs corrects for differences in the effective zeros of the various channels as well as giving an increase in sensitivity.

The degree of linear polarization p and the polarization position angle χ are given by

$$p = (Q^2 + U^2)^{1/2}/I \quad \text{and} \quad \chi = \frac{1}{2} \tan^{-1}(U/Q). \quad (3)$$

The performance of the linear polarization switching was checked by continuum observations of the polarized source Fornax A and of a nearby comparison region. For the line emission, comparison point observations are not necessary, as the channels outside the line, containing continuum only, provide the reference level.

When both linear and circular components are present the polarization can be considered to comprise an elliptical and a random component. The position angle of the ellipse is still obtained from the linear polarization measurements (equation (3)). The degree of polarization m and the axial ratio given by $\tan \beta = \text{major axis/minor axis}$ are

$$\text{and} \quad \left. \begin{aligned} m &= (Q^2 + U^2 + V^2)^{1/2}/I = (p^2 + r^2)^{1/2} \\ \sin 2\beta &= V/(Q^2 + U^2 + V^2)^{1/2} = r/m. \end{aligned} \right\} \quad (4)$$

IV. RESULTS

(a) *Optical and Radio Continuum Data*

Photographs of the nebula given in Plates 1 and 2 are reproduced from a plate kindly made available by Dr. Roslund of the Uppsala Southern Station at Mount Stromlo Observatory. The radio continuum contours superimposed on Plate 2 were reduced by the present authors from original records of a survey of HII regions carried out by R. W. Clarke and N. W. Broten at the Division of Radiophysics. The wavelength was 11.3 cm, the aerial beamwidth $7' \cdot 5$ arc. Contours at 18 cm wavelength, constructed from the total power records taken simultaneously with the line observations, are consistent with those at 11.3 cm.

The continuum contours in Plate 2 add to our knowledge of the group of nebulae associated with NGC 6334. The two southern bright areas are seen to be separate, whereas the form of the main group of contours indicates that the two northern bright areas must form a single whole with an intense cloud of dark matter causing the apparent dividing lane between them.

(b) OH-line Observations

Figures 1(a) and 1(b) are examples of the profiles in the direction of NGC 6334 observed at 1665 MHz with the linearly polarized feed and frequency switching. In Figure 1(a) two emission peaks near -12 and -8.5 km/sec can be distinguished, while there is absorption centred at -4.5 km/sec.

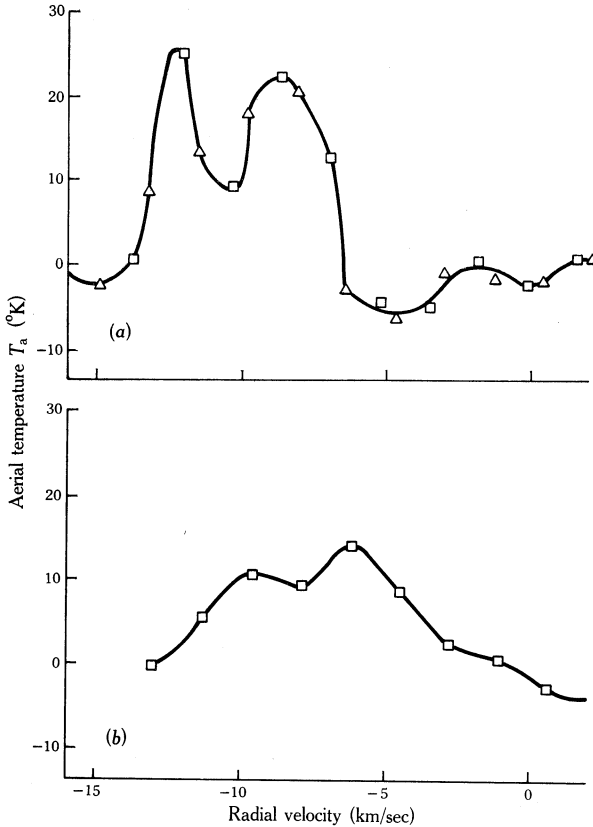


Fig. 1.—OH-line profiles of NGC 6334 observed at 1665 MHz with a bandwidth of 10 kHz. (a) Profiles taken in the direction R.A. $17^{\text{h}} 18^{\text{m}} 32^{\text{s}}$, Dec. $-35^{\circ} 42' \cdot 5$ (1966.2), near the maximum of source A. Two series of observations are indicated with different symbols. (b) Profiles taken in the direction R.A. $17^{\text{h}} 17^{\text{m}} 32^{\text{s}}$, Dec. $-35^{\circ} 52' \cdot 5$ (1966.2), near the maximum of source B.

Profiles were taken at 50 points at approximately half-beamwidth spacings across the nebula at 1665 MHz. The distribution of intensity and velocity was found to be consistent with two point sources, A and B (Plate 2). They are $\sim 16' \cdot 5$ arc apart and so are completely resolved with the $12' \cdot 2$ beam of the 210 ft radio telescope. Figures 1(a) and 1(b) are profiles taken near A and B respectively.

At 1667 MHz the same two centres of emission were found. Profiles near A and B are shown in Figures 2(a) and 2(b), and a comparison with Figures 1(a) and 1(b) reveals that B is now the stronger source, whereas A was stronger at 1665 MHz. In addition, each source now has only a single velocity peak, the values of which, -10.6 km/sec for A and -9.3 km/sec for B, are intermediate between the multiple peaks observed at 1665 MHz.

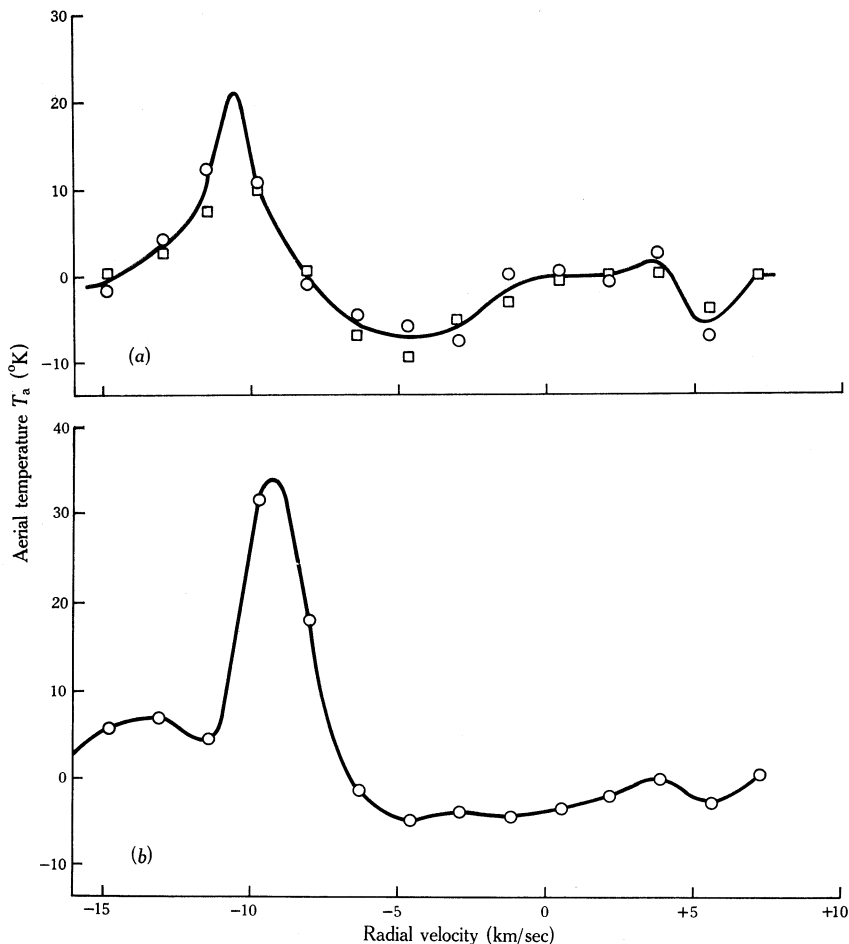


Fig. 2.—OH-line profiles of NGC 6334 observed at 1667 MHz. (a) Profiles taken in the direction R.A. $17^{\text{h}} 18^{\text{m}} 32^{\text{s}}$, Dec. $-35^{\circ} 47' \cdot 5$ (1966.2), near the maximum of source A. (b) Profiles taken in the direction R.A. $17^{\text{h}} 17^{\text{m}} 32^{\text{s}}$, Dec. $-35^{\circ} 52' \cdot 5$ (1966.2), near the maximum of source B.

The absorption features, similar at 1667 and 1665 MHz, are centred on -4.5 and $+5.5$ km/sec (the latter being outside the range of the profiles given in Fig. 1). The absorption maximum, however, occurs near the maximum of the continuum radiation at $17^{\text{h}} 18^{\text{m}} 10^{\text{s}}$, $-35^{\circ} 48' \cdot 0$ (1966.2), approximately midway between A and

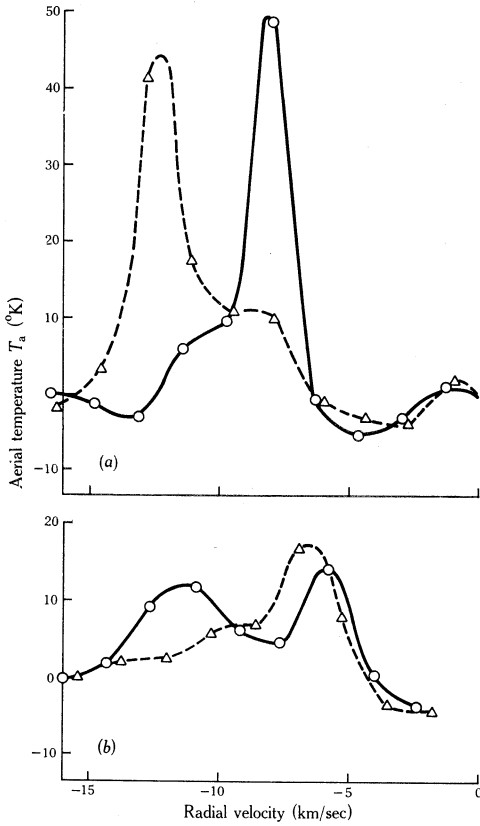


Fig. 3.—OH-line profiles, (a) corresponding to Figure 1(a) and (b) corresponding to Figure 1(b), showing the circular polarization components; sense is right-handed in the dashed curves and left-handed in the full curves.

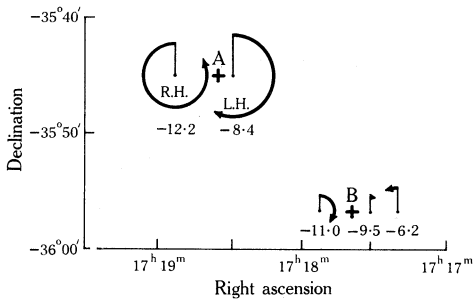


Fig. 4.—Schematic representation of the circular polarization characteristics of sources A and B at 1665 MHz. The degree of polarization r is represented by the segment of an arc of a circle whose radius is proportional to $I_{RHC} + I_{LHC}$ (i.e. to the total intensity). The directions of the arrows indicate the sense; anticlockwise is R.H.C, clockwise L.H.C. The value of the radial velocity (km/sec) is shown under each segment.

B. At 1665 MHz the apparent opacities, defined as the ratio of the absorption line intensity to the 18 cm continuum intensity, were 0.10 at -4.5 km/sec and 0.05 at $+5.5$ km/sec. The 1667/1665 ratio of the absorption lines at -4.5 km/sec agrees approximately with the theoretical value of 9/5. The velocity range near $+5.5$ km/sec was not covered completely at 1667 MHz. The range of the -4.5 km/sec absorption was from 0 to -6.5 km/sec, although it is possible that it extends to more negative velocities but is masked by the emission.

TABLE 1
DISTRIBUTION OF CIRCULAR POLARIZATION OF OH-LINE EMISSION AT 1665 MHz FROM SOURCES A
AND B OF NGC 6334

Position (1966.2)					Radial Velocity (km/sec)	I_{RHC} I_{LHC} (computer units)		Circular Polarization	
R.A. h m s	Dec. ° ' "					$ r $	Sense		
Source A									
17 18 02	-35	47.5	-8.2	30	51	0.41	LH		
			-11.3	70	13	0.69	RH		
17 18 16	-35	47.5	-8.1	30	102	0.54	LH		
			-12.2	91	8	0.84	RH		
17 18 32	-35	42.5	-8.1	32	144	0.64	LH		
			-12.4	128	1	0.99	RH		
17 18 32	-35	47.5	-8.4	50	129	0.44	LH		
			-12.0	107	25	0.62	RH		
17 18 32	-35	52.5	-8.4	22	68	0.51	LH		
			-12.6	39	0	1.00	RH		
17 19 02	-35	47.5	-8.4	14	92	0.74	LH		
			-11.5	70	9	0.77	RH		
Means			-8.4			0.55 ± 0.15	LH		
			-12.2			0.82 ± 0.20	RH		
Source B									
17 17 32	-35	47.5	-6.0	15	12	0.11	RH		
			-9.0	11	18	0.24	LH		
			-12.0	10	10	0	—		
17 17 32	-35	52.5	-6.4	50	42	0.11	RH		
			-9.5	20	21	0.02	LH		
			-11.3	10	36	0.57	LH		
17 17 32	-35	57.5	-6.2	42	52	0.11	LH		
			-9.5	37	26	0.17	RH		
			-11.0	23	38	0.25	LH		
17 17 32	-36	02.5	-6.0	22	17	0.13	RH		
			-9.0	11	11	0	—		
			-10.6	6	26	0.63	LH		
Means			-6.2			0.06 ± 0.04	RH		
			-9.5			0.02 ± 0.06	LH		
			-11.0			0.36 ± 0.12	LH		

(c) Circular Polarization (1665 MHz)

Examples of the profiles observed with the circularly polarized feeds are given in Figures 3(a) and 3(b) for the positions shown in Figures 1(a) and 1(b) respectively for linearly polarized feeds. The LHC profiles are shown as continuous curves and the RHC as dashed curves. The striking feature of Figure 3(a) is the fact that source A has only a single velocity peak for each polarization. The distributions of the circularly polarized intensities were still consistent with the existence of the same

two centres A and B of emission. An attempt has been made in Figure 4 to illustrate the polarization characteristics of the radiation from A and B. The degree of polarization r is represented by the segment of an arc of a circle whose radius is proportional to the sum of I_{RHC} and I_{LHC} , that is, to the total intensity I . The direction of the arrows indicates the sense (anticlockwise is RHC and clockwise LHC). The radial velocity is shown under each segment.

Table 1 lists the positions at which observations of circular polarization were made and the degree of circular polarization derived for each point. Variations are mainly due to sensitivity limitations, and averages are given for sources A and B at each of the velocity peaks. No circular polarization measurements were made at 1667 MHz.

TABLE 2
LINEAR POLARIZATION FOR SOURCE A OF NGC 6334
Measurements centred on $17^{\text{h}} 18^{\text{m}} 16^{\text{s}}$, $-35^{\circ} 45' \cdot 0$, and made on March 12–13, 1966

OH-emission Line (MHz)	Radial Velocity (km/sec)	Linear Polarization p (%)	Position Angle χ (degrees)
1667	-12 to -7	< 5	—
1665	-11·8	7 ± 4	120 ± 20
1665	-10·1*	10 ± 3	90 ± 15
1665	-8·4†	4 ± 2	75 ± 20

* Also one observation of $p \sim 20\%$ (see text).

† Compare with $p = 24\cdot5\%$, $\chi = 70^{\circ}$, obtained by grouping five of the 2 kHz channels near No. 42 in Williams, Dieter, and Weaver (1966).

(d) Linear Polarization

Linear polarization measurements were restricted to source A and were made over a grid of points (± 15 sec in right ascension, $\pm 2' \cdot 5$ in declination) centred on $17^{\text{h}} 18^{\text{m}} 16^{\text{s}}$, $-35^{\circ} 45' \cdot 0$ (1966·2). Table 2 summarizes the information from observations made between March 12 and 14, 1966. At 1665 MHz the degree of linear polarization p is below 10% between -12 and -8 km/sec, apart from a single transient increase to a maximum of 20% at -10 km/sec. This subsequently fell to below 10% in a further observation 2 hr later. Such an occurrence would normally be regarded as spurious, but it is noted here in view of the reports of secular variation.

Williams, Dieter, and Weaver (1966) have reported large amounts of linear polarization in the 1665 MHz radiation from NGC 6334 when observed with 2 kHz bandwidth. Their values for a radial velocity of -8·6 km/sec were averaged over 5×2 kHz channels and are given as a footnote to Table 2 for comparison with the present results.

At 1667 MHz the linear polarization in the vicinity of source A was below 5%. The OH-line absorption appears to be unpolarized ($< 15\%$) at both frequencies.

To summarize, we find that our observations indicate that linear polarization of the OH-emission from source A is insignificant with a bandwidth of 10 kHz.

(e) Positions and Intensities of the OH-line Emission Sources

The positions of the centres of sources A and B have been estimated from the mapping observations at 1665 and 1667 MHz with linearly and circularly polarized feeds. More points are available from the former, but the latter consist of more intense values, so that equal weight is attached to each set. Each estimate of position is listed in Table 3. The average position for the maximum in source A is $17^{\text{h}}17^{\text{m}}32^{\text{s}}$, $-35^{\circ}43' \cdot 8$ (1950), with maximum deviations of ± 2 sec in right ascension and

TABLE 3

SUMMARY OF POSITION INFORMATION AND INTENSITIES OF OH-LINE EMISSIONS FROM NGC 6334

Type of Observation	Radial Velocity of Line Peak (km/sec)	Position (1966.2)					Maximum Intensities (°K)
		R.A.			Dec.		
		h	m	s	°	'	
Source A							
Mapping 1665 MHz	-12.0	17	18	36	-35	43.8	27
	-8.4	17	18	36	-35	45.3	34
Mapping 1667 MHz	-10.6	17	18	32	-35	45.5	17
	—	—	—	—	—	—	0
Circular polarization 1665 MHz	-12.2	17	18	33	-35	45.0	
	-8.4	17	18	37	-35	44.5	
Average position of centre		17	18	35	-35	44.8	
Precessed to 1950.0		17	17	32	-35	43.8	
Maximum departures				± 2		$+0.7 - 1.0$	
Source B							
Mapping 1665 MHz	-9.5	17	17	41	-35	57.7	19
	-6.2	17	17	35	-35	57.0	25
Mapping 1667 MHz	-13.0	17	17	42	-35	56.0	10
	-9.3						49
Circular polarization 1665 MHz	-11.0	17	17	36	-35	55.0	
	-6.2						
Average position of centre		17	17	38	-35	56.4	
Precessed to 1950.0		17	16	34	-35	55.4	
Maximum departures				± 3		$+1.3 - 1.4$	

$+0.7$, -1.0 , in declination. For source B the average position is $17^{\text{h}}16^{\text{m}}34^{\text{s}}$, $-35^{\circ}55' \cdot 4$ (1950.0), with maximum deviations of ± 3 sec in right ascension and $+1.3$, -1.4 , in declination. The errors are about twice the pointing errors of the radio telescope. We cannot be certain that the individual positions are really distinct or are just the result of errors of observation.

Sources A and B are on either side of the continuum maximum and at points of equal continuum intensity (see Plate 2), 38°K aerial temperature at 1660 MHz. They lie on a line approximately parallel to the galactic equator.

The maximum emission line intensities obtained from the plotting of the mapping observations are given in the final column of Table 3. At 1665 MHz, source A is more intense than source B, but at 1667 MHz the -9.3 km/sec component in source B is the most prominent of all. In source A at 1665 MHz emission greatly exceeds that at 1667 MHz; in source B the integrated 1667 MHz emission is 50% more intense than the 1665 MHz.

(f) *Secular Variations*

The observations, which were made in one period in 1965 and in two in 1966, do not indicate large variations of intensity.

V. DISCUSSION

(a) *The Location of the Absorbing Gas*

The following considerations support the idea that the absorption features in the profiles are due to hydroxyl molecules in two gas complexes between NGC 6334 and the Sun and possibly at considerable distances from the nebula.

The velocities of the OH-absorption features at -4.5 and $+5.5$ km/sec agree within the experimental errors with the velocities of the two absorption features in neutral hydrogen observed by Clark, Radhakrishnan, and Wilson (1962) at -5.7 and $+4.2$ km/sec. The optical depths of the H-line absorptions are $\tau \approx 1$. Simple calculations show that the hydrogen complexes would have to extend several hundred parsecs in the line of sight unless the hydrogen density is greater than, say, 5 cm^{-3} .

Now the direction of NGC 6334, $l^{\text{II}} = 351^\circ$, is not favourable for the estimation of distance from the galactic rotation model (e.g. Kerr and Westerhout 1965), but a reasonable estimate of 600 pc could be placed on the gas represented by the -5 km/sec velocity. The positive velocity, $+4.2$ km/sec, is in a wide hydrogen absorption line profile and cannot be located by this means. It is possibly in the solar neighbourhood, say, at 200 pc distance. Each estimate is considerably less than 1300 pc, the distance to the nebula given by Roslund (1966).

Additional information on the location of the absorbing OH comes from the nebula NGC 6357, which, at $l^{\text{II}} = 353^\circ$, is only 2° away from NGC 6334. The OH-absorption features are again two, at radial velocities -5.8 and $+5.3$ km/sec (McGee, Gardner, and Robinson 1967). The apparent opacities are approximately the same for both nebulae. For NGC 6357, Clark, Radhakrishnan, and Wilson (1962) have observed a more complex H-line absorption profile, which nevertheless has its two most prominent features near these velocities. The optical depths are approximately the same as for NGC 6334 within the errors given.

On the other hand, recent observations of the $\text{H}_{126\alpha}$ recombination line (McGee and Gardner 1967) show that the line is centred at a radial velocity of -4 km/sec for NGC 6334 with a half-intensity range of -20 to $+11$ km/sec; for NGC 6357 corresponding values are $+7$ km/sec and -20 to $+14$ km/sec. The large line widths are considered to be mainly due to high temperatures and turbulence. However, because the OH-absorption occurs in two discrete velocity ranges each 3.4 km/sec wide, and because the opacity is uniform across the source, we favour the view that the absorbing gas is well away from the nebula.

(b) The Location of the Emitting OH-gas

As will be mentioned in the following section, the nature of the OH-line emission requires it to be closely associated with the HII region. From the galactic rotation model a distance estimate for the average gas velocity of about -10 km/sec is close to 1300 pc, the distance of NGC 6334.

In Plates 1 and 2 sources A and B are seen to lie in a lane of dark matter that stretches across the group of nebulae in a line parallel to the galactic equator (at approximately $b^{\text{II}} = +0^{\circ}40'$). The sources are $16' \cdot 5$ arc apart or $6 \cdot 2$ pc for the distance just given.

(c) Possible Patterns in the OH-line Emission

There are a number of features of the emission that may have some bearing on the mechanisms involved. They are:

- (1) At 1665 MHz the median velocity, -10 km/sec, associated with source A is 2 km/sec more negative than the velocity of B, -8 km/sec. At 1667 MHz there is a similar difference between the components; A has a median velocity of $-10 \cdot 6$ and B of $-9 \cdot 6$ km/sec. Thus the velocity difference probably indicates some motion of that part of the nebula or dust associated with the OH-emission, e.g. rotation.
- (2) The velocity spread of the emission is greater at 1665 than at 1667 MHz for each source. The 1667 peak velocities are located between those for 1665.
- (3) At 1665 MHz for source A the most negative velocity at ~ -12 km/sec is RHC, the most positive velocity at ~ -8 km/sec is LHC. For source B the situation is reversed (see Fig. 4), although the degree of polarization and also the emission are considerably lower. At 1667 MHz source B is the more intense, but no information is at present available on its circular polarization.

(d) Comparison with Other Observations of Polarization

Prior to this communication it was difficult to reconcile two sets of polarization observations. Williams, Dieter, and Weaver (1966) noted linear polarization in NGC 6334 approaching $p = 100\%$, which would exclude substantial circular polarization. On the other hand, Barrett and Rogers (1966) had found strong circular polarization in the OH-line emission.

In Section IV our measurements on both types of polarization show that circular polarization is present in considerable proportions and linear polarization is scarcely discernible. In addition, we have a series of earlier observations, made in August–September 1965 over a range of position angles, that did not reveal large amounts of linear polarization. However, some linear polarization could be accounted for if the $-7 \cdot 5$ km/sec component in source B (not observed by us for linear polarization) were, in fact, 100% linearly polarized. (We do know that its degree of circular polarization is low.) If source B were 100% linearly polarized, an observation with an 85 ft dish, which would include both components in the beam, might yield some 50% linear polarization.

VI. ATTEMPTS TO EXPLAIN THE OBSERVED EMISSION

We shall conclude by relating the known experimental facts to the various theories that have been proposed to explain the anomalous OH-emission.

The emitting molecules are found to be localized near the edge of HII regions. The small sizes of the emitting sources imply a very high brightness temperature T_b . The limits on source size from interferometer observations (Cudaback, Read, and Rougoor 1966; Rogers *et al.* 1966) lead to angular size under $20''$ arc and T_b as high as 10^6 °K. This contrasts with the sharpness of the emission lines. The typical width, $\Delta\nu$, of 2 kHz would, at its face value, correspond to a kinetic temperature of under 50 °K.

High temperatures and narrow line widths can be most easily reconciled if the populations of the OH-states are inverted and amplification of the background radiation (at most some tens of degrees Kelvin) takes place. The power gain G required is then typically 10^4 – 10^5 , which would produce a narrowing of the line width by a factor of $(\log 2)/\log(\frac{1}{2}G)^{\frac{1}{2}} \approx \frac{1}{5}$. Thus an observed 2 kHz width could correspond to a true Doppler spread of 10 kHz or a kinetic temperature of several hundred degrees in the absence of turbulence or streaming. There are reasons for believing that the temperature in the region might be well below this.

A high power gain requires a considerable number of molecules in the line of sight with a small velocity spread, plus an efficient process for population inversion. If T_c is the brightness temperature of the continuum background and T_1 the temperature at the peak of the emission line, the equation of transfer yields (neglecting spontaneous emission)

$$\begin{aligned} \log(T_1/T_c) &= \frac{c^2}{8\pi\nu^2} \frac{A_{21}}{\Delta\nu} \int \{n_2 - (g_2/g_1)n_1\} ds \\ &= \frac{9 \cdot 1 \times 10^{-10}}{\Delta\nu} \int \{n_2 - (g_2/g_1)n_1\} ds, \end{aligned}$$

at 1665 MHz, where $A_{21} = 7 \cdot 1 \times 10^{-11}$ sec $^{-1}$, $\Delta\nu$ is the line width, n_i is the population of level i , and g_i is the statistical weight of level i . If we take $\log(T_1/T_c)$ approximately equal to 10, then

$$\int \{n_2 - (g_2/g_1)n_1\} ds = 10^{14} \text{ cm}^{-2} \quad \text{for } \Delta\nu = 10 \text{ kHz.}$$

If the depth of the emitting region were comparable with its angular size of about 0.1 pc, we would require

$$\{n_2 - (g_2/g_1)n_1\} \approx 3 \cdot 6 \times 10^{-4} \text{ cm}^{-3}.$$

For microwave transitions an inversion of 1% would require a most efficient process, and we would then need $n_2 \approx 0 \cdot 03$ cm $^{-3}$ to give the gain required. If the oxygen molecules have the normal abundance, 1/1700, and a fraction α have formed hydroxyl molecules, we thus require about $50/\alpha$ hydrogen atoms per cubic centimetre. It should also be mentioned that if the absorption is enhanced in certain directions through the nebula ("anti-maser" effect) these patches of increased absorption would not be detected, since their maximum T_b of ~ 10 °K would be insignificant beside the emission T_b of 10^6 °K.

The most satisfactory method yet proposed for producing the population inversion appears to be "pumping" by the ultraviolet radiation associated with the HII region (Cook 1966a; Perkins, Gold, and Salpeter 1966). Cook has suggested that the OH-inversion is probably restricted to a narrow shell near the ionization front of the HII region. The number of molecules in the line of sight will be a maximum near the periphery of the shell and for the idealized case of a spherical shell the emission will have the form of a circular ring. This annular concentration will be enhanced by the fact that it is $\log T_1$ that is proportional to the total number of molecules in the line of sight, and by the fact that in this direction the dispersion of expansion velocities (Mathews 1965) is not seen.

In NGC 6334 we observe two centres of OH-emission near the periphery of the largest of the group of nebulae and apparently in a dust lane. As a complete ring is not seen, we can infer that the inversion process is much more selective than those so far proposed or, alternatively, that the OH-density is not uniform. It has been suggested that the rate of formation of OH-molecules will increase in the presence of dust, and thus the density would be greatest along the dust lane. The ring would then be replaced by a double source, with components separated along the dust lane.

The pattern of the polarization splitting suggests the presence of a longitudinal component of magnetic field. An examination of the Zeeman patterns for 1665 and 1667 MHz, given as Figure 8 by Williams, Dieter, and Weaver (1966), shows that to a first approximation a triple splitting occurs at both frequencies but that the separation of the σ -components is considerably greater for 1665 than for 1667 MHz: 3.24 compared with 1.96 MHz/G. In Section V we noted that the 1665 emission covered a wider range of frequencies than the 1667. If this is not just fortuitous, magnetic fields exceeding 10^{-3} G are required to explain a difference in width of ~ 1 km/sec (= 5 kHz). It is possible to obtain appreciable circular polarization at 1665 MHz with a lower field if we only require a magnetic splitting of the order of the width of the individual components. For $\Delta f = 500$ Hz, a longitudinal field of 2×10^{-4} G would suffice. If such fields were present, it would be improbable that the emission of the two σ -components with RHC and LHC polarizations would be equal, as small gradients in velocity along the line of sight would favour either one or the other component (Cook 1966b). For a magnetic field directed towards the observer but decreasing in intensity as the velocity (also towards observer) increases, the polarization will be RHC. On this picture the individual polarization components and the different frequencies will have slightly different positions. The present observations are not capable of demonstrating whether this is so, but it is within the range of future interferometer studies.

The main difficulty with this simple picture is that large magnetic fields are required. With the compression of a spiral arm field by the ionization front an upper limit of around 10^{-4} G might be attained under the most favourable circumstances. Fields exceeding this are only possible if rotation and winding-up of field lines takes place (Piddington, personal communication). If the dark obscuring matter were rotating, this might conceivably occur.

Alternative explanations for circular polarization in terms of maser saturation have been proposed by Heer (1966) and Litvak *et al.* (1966). While these have an

advantage in not requiring such high fields, they do require larger numbers of OH-molecules along the line of sight.

VII. ACKNOWLEDGMENTS

The authors wish to thank Miss Jan Milton and Miss Mary Chapman for considerable help in data processing. They acknowledge the detailed discussions during observations with Mr. V. Radhakrishnan. With pleasure they thank Dr. R. H. Turrin of the Bell Telephone Laboratories, Holmdel, New Jersey, U.S.A., who supplied the design of feed 2.

VIII. REFERENCES

- BARRETT, A. H., and ROGERS, A. E. E. (1966).—*Nature, Lond.* **209**, 188–90.
- BOLTON, J. G., GARDNER, F. F., and MACKEY, M. B. (1964).—*Aust. J. Phys.* **17**, 340–72.
- CLARK, B. G., RADHAKRISHNAN, V., and WILSON, R. W. (1962).—*Astrophys. J.* **135**, 151–74.
- COOK, A. H. (1966a).—*Nature, Lond.* **210**, 611.
- COOK, A. H. (1966b).—*Nature, Lond.* **211**, 503.
- CUDABACK, D. D., READ, R. B., and ROUGOOR, G. W. (1966).—*Phys. Rev. Lett.* **17**, 452–5.
- DIETER, NANNIELOU H., WEAVER, H., and WILLIAMS, D. R. W. (1966).—*Astr. J.* **71**, 160.
- GARDNER, F. F., and DAVIES, R. D. (1966).—*Aust. J. Phys.* **19**, 441–59.
- GARDNER, F. F., and WHITEOAK, J. B. (1966).—*A. Rev. Astr. Astrophys.* **4**, 245–92.
- HEER, C. V. (1966).—*Phys. Rev. Lett.* **17**, 774–5.
- KERR, F. J., and WESTERHOUT, G. (1965).—In “Stars and Stellar Systems”. (Eds. A. Blaauw and M. Schmidt.) Vol. 5, pp. 167–202. (Chicago Univ. Press.)
- LITVAK, N. M., McWHORTER, A. L., MEEKS, M. L., and ZEIGER, H. J. (1966).—*Phys. Rev. Lett.* **17**, 821–6.
- MCGEE, R. X., and GARDNER, F. F. (1967).—*Nature, Lond.* **213**, 579.
- MCGEE, R. X., GARDNER, F. F., and ROBINSON, B. J. (1967).—OH observations in the directions of galactic thermal sources. *Aust. J. Phys.* **20** (in press).
- MCGEE, R. X., and MURRAY, J. D. (1963).—*Proc. Instn Radio Engrs Aust.* **24**, 191–6.
- MCGEE, R. X., ROBINSON, B. J., GARDNER, F. F., and BOLTON, J. G. (1965).—*Nature, Lond.* **208**, 1193–5.
- MATHEWS, W. G. (1965).—*Astrophys J.* **142**, 1120.
- PERKINS, F., GOLD, T., and SALPETER, E. E. (1966).—Cornell–Sydney University Astronomy Centre, Rep. No. 40.
- ROGERS, A. E. E., *et al.* (1966).—*Phys. Rev. Lett.* **17**, 450–2.
- ROSLUND, C. (1966).—*Ark. Astr.* **4**, 101–22.
- WEAVER, H., WILLIAMS, D. R. W., DIETER, N. H., and LUM, W. T. (1965).—*Nature, Lond.* **208**, 29–31.
- WEAVER, H., WILLIAMS, D. R. W., DIETER, NANNIELOU, H. (1966).—*Astr. J.* **71**, 184.
- WILLIAMS, D. R. W., DIETER, NANNIELOU, H., and WEAVER, H. (1966).—*Astr. J.* **71**, 186.